Eu-Doped GaN Films Grown by Phase Shift Epitaxy

Mingyu Zhong and Andrew J. Steckl*

Nanoelectronics Laboratory, University of Cincinnati, Cincinnati, OH 45221-0030, U.S.A.

Received October 15, 2010; accepted November 10, 2010; published online December 3, 2010

Phase shift epitaxy (PSE) is a dynamic thin film growth technique wherein constituent fluxes are pulsed with an adjustable phase shift. PSE enables the introduction of dopants during the optimum segment of the growth cycle. Eu-doped GaN films were grown with Ga and Eu shutters periodically opened and closed (with varying phase shift) while keeping N flux constant, so that the Ga and Eu coverage on surface during each cycle varies in a controlled way. The Eu concentration and photoluminescence (PL) efficiency are strongly influenced by the PSE parameters. Eu ions doped during high Ga coverage exhibit strong PL efficiency. © 2010 The Japan Society of Applied Physics

DOI: 10.1143/APEX.3.121002

Rare earth (RE) doped GaN materials have been investigated[1–3] for their strong and narrow photo-emission lines at visible and IR wavelengths and associated photonic applications. Generally, GaN:RE films are grown by molecular beam epitaxy (MBE) using metallic sources for the REs and group III metals and a N_2 plasma source. Eu-doped GaN and related light emitting devices have been investigated[4–10] because of their strong red emission of ~620 nm. N-rich conditions promote RE incorporation,[11] while the slightly Ga-rich condition (which results in the best crystal quality) is favorable for RE luminescence efficiency (ratio of photoluminescence to RE concentration).

The use of fluxes modulated with time (alternating group III and group V), known as flow rate modulation epitaxy (FME), has been shown to improve the semiconductor material quality in the chemical vapor deposition growth of GaAs,[12] GaN,[13] and other III/V compounds, leading to high quality structures and devices.[14] Similar improvements have been reported in the MBE growth of GaAs[15] and GaN[16] with the equivalent technique of migration enhanced epitaxy (MEE). Impurity doping with these modulated growth techniques have also been investigated. Munasinghe and Steckl[17,18] have reported a ~10× enhancement of Eu^{3+} luminescence in GaN by interrupted growth MBE. Recently, a similar MBE pulsed growth technique — metal modulated epitaxy (MME) — has been reported[19–22] to enhance the conductivity of p-type Mg doped GaN. In MME, metal fluxes (Ga, Mg) are modulated simultaneously for very short periods (~5–10 s) in both open and closed configurations, while maintaining continuous N_2 plasma. Extremely high Ga-rich condition is used to smooth the surface during the metal shutter ON period. During the metal shutter OFF period, N_2 fully saturates the film to prevent droplet buildup. High Mg doping efficiency and high hole concentrations were achieved in GaN:Mg thin films grown by the MME technique.

In this paper, a generalized time-varying growth technique — *phase shift epitaxy* (PSE) — is introduced and is applied to the growth of GaN:Eu films. The basic approach (illustrated in Fig. 1) utilizes an additional degree of freedom: the overlap between the leading (x) and tailing (z) edges of the metal (Ga and Eu) fluxes. The MME approach (Ga and Eu fluxes simultaneously pulsed) can seen to be a special case of PSE, where x and z are equal to zero. In both techniques, the N flow is continuous.

*E-mail address: a.steckl@uc.edu

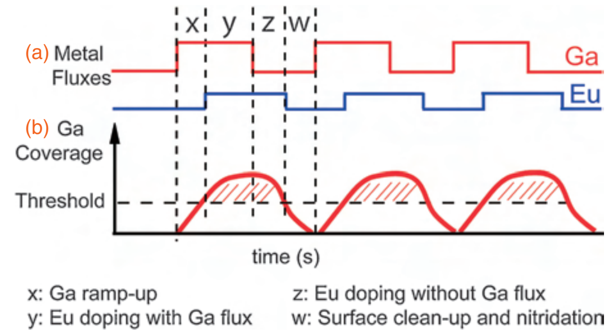

Fig. 1. Diagrams describing the operation of phase shift epitaxy applied to Eu-doped GaN growth: (a) Ga and Eu fluxes during actual PSE cycles; (b) Ga coverage on the surface during PSE cycles.

Eu-doped GaN films were grown on AlGaN templates on p-Si(111) wafers (Nitronex). Films grown by PSE were compared to films grown by conventional MBE and to films where only the Ga flux was pulsed. The substrate temperature was 650 °C and the N_2 plasma operated at 1 sccm and 300 W. The Eu cell temperature was 420 °C.

PSE films were grown with a Ga cell temperature of 900 °C, resulting in a beam equivalent pressure (BEP) of 4.4×10^{-7} Torr. This corresponds to the III/V ≫ 1 case in conventional MBE. A single cycle of 22 s consisted of $Ga_{ON} = 14$ s and $Ga_{OFF} = 8$ s. The x-parameter (shift between Ga and Eu leading edge) was varied from 4 to 1 s, while the z-parameter (shift between Ga and Eu trailing edge) was varied from 3 to 6 s. A second set of samples was grown with continuous Eu flux, while the Ga flux was pulsed with a constant $Ga_{ON} = 14$ s and several values of $Ga_{OFF} = 8, 10, 12$ s. Finally, a third set of films were grown by conventional MBE with various III/V ratios.

The MBE growth time was 23 min. PSE films had an equivalent Ga growth time spread over 90 cycles of 14 s each. Films from all the three sets had a very similar thickness of ~150 nm. This allows the direct comparison of the photoluminescence (PL) emission and PL efficiency from samples grown under different conditions.

Secondary ion mass spectroscopy (SIMS) was used to determine the Eu depth profile and calculate Eu atomic concentrations. PL measurements were performed at 25 °C with a 325 nm He–Cd laser.

Four MBE samples were grown with different III/V ratios (from ≪1 to ≫1), as shown in Fig. 2. As previously reported[11] the Eu concentration decreases monotonically with increasing Ga flux because of site competition in the

 © 2010 The Japan Society of Applied Physics

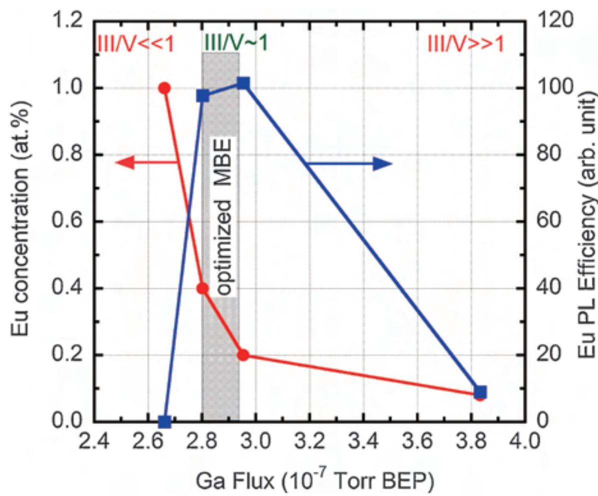

Fig. 2. GaN:Eu film grown by conventional MBE: Eu concentration and PL efficiency with different Ga fluxes.

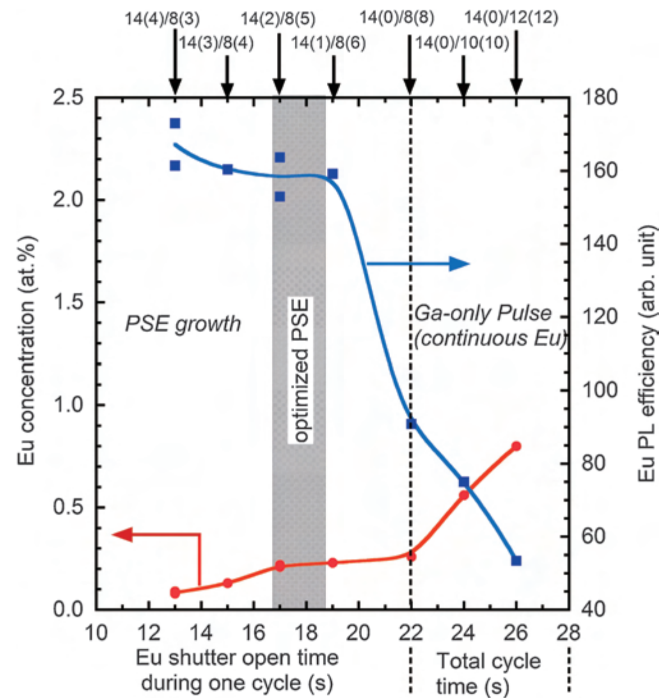

Fig. 3. GaN:Eu films grown by PSE: Eu concentration and PL efficiency obtained for different Eu shutter open times. PSE conditions for each sample are labeled on the top horizontal axis: $Ga_{ON}(x)/Ga_{OFF}(z)$.

group III sublattice of the GaN film. The Eu PL efficiency is calculated by dividing the integrated PL of the Eu peaks around 620 nm by the product of the Eu concentration and the film thickness. The highest efficiency is obtained at III/V $\cong$ 1 (Ga beam pressure of 2.95×10^{-7} Torr).

In *conventional* Ga-rich MBE, Eu atoms are prevented from easily reaching the growth front by the Ga monolayer that is built up during growth. In the N-rich case, the growth front only partially covers the surface, with the uncovered part of the surface being exposed to both N and Eu fluxes. This results in a film with high Eu concentration, but low Eu PL efficiency.

In the PSE approach, the Ga coverage varies during each segment of the cycle. Hence, the effect of each segment can be adjusted. As shown qualitatively in Fig. 1(b), during the Ga_{ON} segment $(x + y)$ the Ga concentration increases. However, the Eu flux is not turned on until sometime after the turn-on of the Ga beam (x-segment). This allows the Ga concentration to build up to a threshold level (III/V $\geq$ 1) before the Eu incorporation process starts. When the Ga pulse is terminated, Eu doping is still allowed (z-segment) until the Ga surface concentration drops below the threshold. During the final component of the PSE scheme (w-segment) both the Ga and Eu fluxes are turned off. During this period, the N beam removes excess Ga from the surface.

Results from the flux time sequence shown in Fig. 1(a) with different phase shifts between the Ga and Eu waveforms are shown in Fig. 3. The PSE scheme is denoted by $Ga_{ON}(x)/Ga_{OFF}(z)$, where Ga_{ON} and Ga_{OFF} are the time lengths of the Ga ON and OFF segments, respectively. x and z are the leading and trailing overlaps of the Ga and Eu waveforms, as seen in Fig. 1. For this set of experiments, the Ga_{ON} and Ga_{OFF} segments are 14 and 8 s, respectively, for a total cycle of 22 s. The Ga_{OFF} segment is used to consume the Ga left on surface so that another cycle can start with "zero" Ga coverage. The x values range from 4 to 1 s and the z values from 3 to 8 s. This set of x and z values leads to a gradually increasing Eu_{ON} time, from 13 to 22 s. In turn, this results in a gradually increasing Eu concentration from 0.13 to 0.23 at.%. At the same time, for shutter times from 13 to 19 s, the efficiency experiences a slight decrease. However, for the Eu shutter time of 22 s [14(0)/8(8)] the PL efficiency experiences a sharp decrease. This is not unexpected since in this case the Eu flux is on continuously and therefore a much greater amount of Eu is incorporated during the w-segment (very low Ga coverage) of the cycle.

Increasing the total cycle time from 22 to 26 s by extending the Ga_{OFF} time and keeping the Eu flux on continuously (in other words Eu shutter time/cycle = $Ga_{ON} + Ga_{OFF}$) results in a sharper increase in Eu concentration and a continuing sharp decrease in Eu PL efficiency. For the Ga_{OFF} time of 8 s (cycle time of 22 s), a 1×1 reflection high energy electron diffraction (RHEED) pattern persists throughout the growth. However, for longer Ga_{OFF} times, the RHEED pattern disappeared shortly after the start of the growth, indicating that longer Ga_{OFF} segments lead to poor crystal quality. As shown in Fig. 3, for these three samples the Eu concentration increased from 0.26 to 0.8 at.% (still well below the concentration quenching limit[5] of Eu of 2.2 at.%), while the PL efficiency dropped from 94 to 54. Clearly, Eu ions incorporated during low Ga coverage suffer from low PL efficiency and these ions also deteriorate the lattice structure. Parameters in the vicinity of 14(1)/8(6) represent optimized PSE conditions.

Compared with optimum conventional MBE samples (dashed region in Fig. 3), the optimum PSE growth (dashed region in Fig. 2) provides a ~50% increase in Eu PL efficiency at approximately the same concentration.

PL spectra in the vicinity of the main Eu intra-4f transition ($^5D_0 \rightarrow {}^7F_2$) obtained from samples grown under several conditions are shown in Fig. 4. The MBE sample grown under optimized conditions (III/V $\approx$ 1) exhibits a large peak at 622.4 nm and a much smaller peak at 620.4 nm. These

 © 2010 The Japan Society of Applied Physics

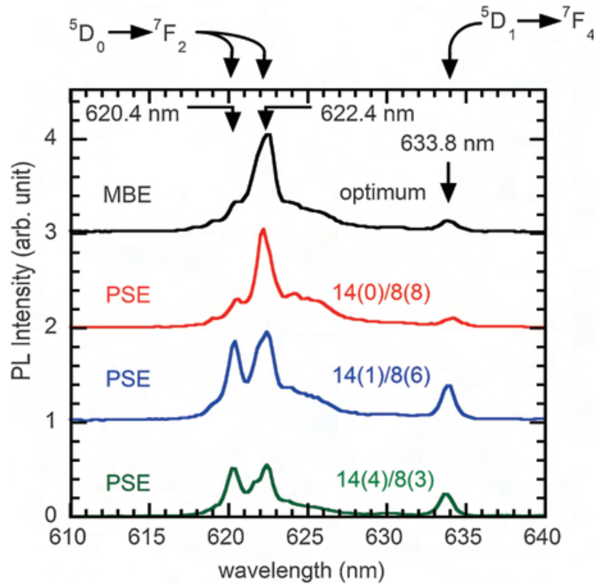

Fig. 4. Eu PL spectra from samples grown under optimum MBE and several PSE conditions.

two peaks have been previously reported[23] and represent the two main Eu incorporation sites. Samples grown under normal PSE conditions (finite phase shift between Ga and Eu waveforms) display greatly enhanced 620.4 nm peak and simultaneously greater PL efficiency. This peak is believed to be from a different Eu site.[14,24,25] The increase of the 620.4 nm peak can be due to a combination of additional Eu incorporation into the second site and reduction of defects that affect the efficiency of this site. The sample grown as the PSE special case with *continuous* Eu flux [14(0)/8(8)] produces a spectrum similar to that of the MBE-grown sample, with the peak at 620.4 nm very much reduced. The sharp decrease of 620.4 nm peak intensity between the 14(1)/8(6) and 14(0)/8(8) samples is probably due to Eu-related defects incorporated during segments of the cycle when Ga coverage is low. This explanation is supported by the gradual disappearance of the RHEED pattern under increasingly low Ga coverage growth conditions [14(0)/10(10) and 14(0)/12(12)]. Furthermore, in the absence of Eu flux, growth under low Ga coverage conditions still exhibits streaking RHEED patterns.

In summary, the PSE growth technique was introduced and applied to the growth of GaN:Eu films. Adjusting the phase shift between metal fluxes during growth enables the incorporation of dopants during the optimum segment of the growth cycle. The PSE technique has the potential to enhance the doping of GaN and of other semiconductors with optoelectronic, magnetic and electronic impurities. This will be very beneficial to applications ranging from lasers to transistors.

Acknowledgments This work is supported in part by a US Army Research Office grant W911NF-10-1-0329. The authors thank R. Wang for initial experiments and J. Roberts for providing the AlGaN templates.

1) A. J. Steckl and J. M. Zavada: MRS Bull. **24** (1999) 33.
2) A. J. Steckl, J. C. Heikenfeld, D. S. Lee, M. J. Garter, C. C. Baker, Y. Q. Wang, and R. Jones: IEEE J. Sel. Top. Quantum Electron. **8** (2002) 749.
3) A. J. Steckl, J. H. Park, and J. M. Zavada: Mater. Today **10** (2007) Nos. 7–8, 20.
4) J. Heikenfeld, M. Garter, D. S. Lee, R. Birkhahn, and A. J. Steckl: Appl. Phys. Lett. **75** (1999) 1189.
5) Z. Q. Li, H. J. Bang, G. X. Piao, J. Sawahata, and K. Akimoto: J. Cryst. Growth **240** (2002) 382.
6) M. Pan and A. J. Steckl: Appl. Phys. Lett. **83** (2003) 9.
7) J. H. Park and A. J. Steckl: Appl. Phys. Lett. **85** (2004) 4588.
8) J. H. Park and A. J. Steckl: J. Appl. Phys. **98** (2005) 056108.
9) K. Wang, R. W. Martin, K. P. O'Donnell, V. Katchkanov, E. Nogales, K. Lorenz, E. Alves, S. Ruffenach, and O. Briot: Appl. Phys. Lett. **87** (2005) 112107.
10) A. Nishikawa, T. Kawasaki, N. Furukawa, Y. Terai, and Y. Fujiwara: Appl. Phys. Express **2** (2009) 071004.
11) R. Wang and A. J. Steckl: J. Cryst. Growth **312** (2010) 680.
12) N. Kobayashi, T. Makimoto, and Y. Horikoshi: Jpn. J. Appl. Phys. **24** (1985) L962.
13) J. J. Huang, K. C. Shen, W. Y. Shiao, Y. S. Chen, T. C. Liu, T. Y. Tang, C. F. Huang, and C. C. Yang: Appl. Phys. Lett. **92** (2008) 231902.
14) Y. Horikoshi: J. Cryst. Growth **202** (1999) 150.
15) Y. Horikoshi, M. Kawashima, and H. Yamaguchi: Jpn. J. Appl. Phys. **25** (1986) L868.
16) D. Sugihara, A. Kikuchi, K. Kusakabe, S. Nakamura, Y. Toyoura, T. Yamada, and K. Kishino: Jpn. J. Appl. Phys. **39** (2000) L197.
17) C. Munasinghe, A. Steckl, E. E. Nyein, U. Hommerich, H. Y. Peng, H. Everitt, Z. Fleischman, V. Dierolf, and J. Zavada: Mater. Res. Soc. Symp. Proc. **866** (2005) 41.
18) C. Munasinghe and A. J. Steckl: Thin Solid Films **496** (2006) 636.
19) S. D. Burnham, W. Henderson, and W. A. Doolittle: Phys. Status Solidi C **5** (2008) 1855.
20) S. D. Burnham, G. Namkoong, D. C. Look, B. Clafin, and W. A. Doolittle: J. Appl. Phys. **104** (2008) 024902.
21) M. Moseley, D. Billingsley, W. Henderson, E. Trybus, and W. A. Doolittle: J. Appl. Phys. **106** (2009) 014905.
22) G. Namkoong, E. Trybus, K. K. Lee, M. Moseley, W. A. Doolittle, and D. C. Look: Appl. Phys. Lett. **93** (2008) 172112.
23) E. E. Nyein, U. Hommerich, C. Munasinghe, A. J. Steckl, and J. M. Zavada: Mater. Res. Soc. Symp. Proc. **866** (2005) 67.
24) E. E. Nyein, U. Hommerich, J. Heikenfeld, D. S. Lee, A. J. Steckl, and J. M. Zavada: Appl. Phys. Lett. **82** (2003) 1655.
25) H. Peng, C. W. Lee, H. O. Everitt, C. Munasinghe, D. S. Lee, and A. J. Steckl: J. Appl. Phys. **102** (2007) 073520.

© 2010 The Japan Society of Applied Physics